

# Identification of the Molecular Parameters that Govern Ordering Kinetics in a Block Copolymer Melt

N. P. Balsara,\* B. A. Garetz,\* M. Y. Chang, H. J. Dai, and M. C. Newstein

*Departments of Chemical Engineering, Chemistry, Materials Science, and Electrical Engineering, Polytechnic University, Six Metrotech Center Brooklyn, New York 11201*

J. L. Goveas

*Materials Research Laboratory University of California, Santa Barbara, California 93106.*

R. Krishnamoorti and S. Rai

*Department of Chemical Engineering, University of Houston, 4800 Calhoun, Houston, Texas 77204*

*Received March 24, 1998; Revised Manuscript Received June 15, 1998*

**ABSTRACT:** The objective of this paper is to identify the molecular parameters that govern ordering kinetics in a diblock copolymer melt. Experimental data on the ordering kinetics were obtained by time-resolved depolarized light scattering after the sample was quenched from the disordered to the ordered state. The ordered state consisted of cylinders arranged on a hexagonal lattice. During the early stages of the disorder-to-order transition, a dilute suspension of ordered grains grow by invading the surrounding, disordered phase. A time-dependent Ginzburg–Landau model was used to relate the growth rate of these grains to molecular parameters. The growth rate is predicted to be proportional to the quench depth and chain radius of gyration and inversely proportional to the molecular relaxation time. Independent estimates of these parameters were obtained from small angle neutron scattering and rheological measurements. The experimentally determined grain growth rates are in good agreement with theoretical predictions, with no adjustable parameters.

## Introduction

A variety of materials are composed of mesophases with periodic concentration profiles.<sup>1–3</sup> Typical examples include block copolymers, surfactant solutions, and eutectic alloys. At high temperatures, entropic factors dominate, and these systems exhibit a homogeneous, liquidlike phase. Repulsive interactions between the components become increasingly important at lower temperatures, and this leads to a symmetry-breaking phase transition to ordered mesophases such as lamellae and cylinders. The forces that drive the formation of the mesophases are well-understood, and a unified framework for studying the equilibrium properties of these seemingly diverse systems has been developed.<sup>3</sup> In contrast, relatively little is known about the kinetics of disorder-to-order phase transitions in these systems.<sup>3</sup>

In this paper we study the ordering kinetics in a block copolymer melt after it was thermally quenched from the disordered state to the ordered state. The size and concentration of the ordered grains were monitored by time-resolved depolarized light scattering experiments. During the early stages of the ordering transition, we found a dilute suspension of ordered grains which grew by consuming the surrounding, disordered phase. The ordering kinetics are characterized by the velocity at which the front of the ordered grains propagates into the disordered phase. We present a time-dependent Ginzburg–Landau model<sup>4</sup> that relates the front propagation velocity during the early stages of grain growth to quench depth, chain radius of gyration, and molecular relaxation time. These parameters were estimated by independent rheological and scattering experiments. We present a quantitative comparison between theory and experiment with no adjustable parameters.

## Experimental Results

A polystyrene-*block*-polyisoprene copolymer was synthesized by anionic polymerization under high vacuum (see ref 5 for details regarding the synthesis and characterization procedures). The weight average molecular weights of the polystyrene and polyisoprene blocks were determined to be 4 and 13 kg/mol, respectively, the polydispersity index of the copolymer = 1.07, and we refer to this polymer as SI(4-13). The polyisoprene block contained 93 mol % 1–4 units and 7% 3–4 units.<sup>5</sup> The equilibrium properties of this sample were obtained from high-resolution X-ray scattering experiments.<sup>6</sup> The block copolymer forms an ordered phase consisting of polystyrene cylinders embedded in a polyisoprene matrix, arranged on a hexagonal lattice. The inter-cylinder spacing is 157 Å, and the cylinder radius is 40 Å. The sample exhibits a disorder-to-order transition at  $59 \pm 1$  °C.<sup>6</sup>

The experiments used to measure ordering kinetics of SI(4-13) are described in refs 7 and 8. The polymer was confined between optical flats and subjected to a series of thermal quenches from the disordered state (70 °C) to the ordered state (below 59 °C). We present results for four quench temperatures: 55.5, 53.7, 52.0, and 50.0 °C. The ordering kinetics were measured by time-resolved depolarized light scattering experiments. Time zero ( $t = 0$ ) is defined as the time at which the quench was initiated. At very early times (ca.  $t < 300$  min), the scattering signal was comparable to that measured in the disordered state. Therefore structural changes that occurred during this period could not be measured. Beyond this point, we observed a marked increase in the depolarized scattering intensity due to rapid grain growth. The relationship between the scattering profiles and grain parameters (size, shape,

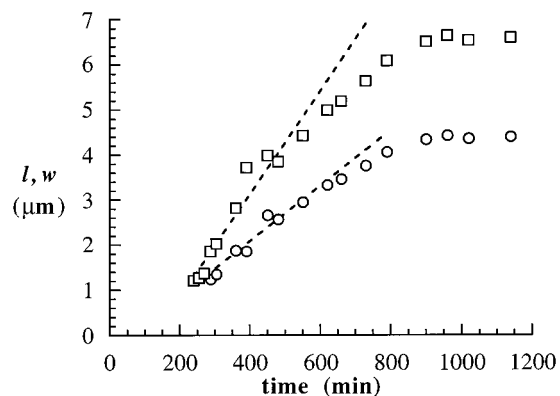


**Figure 1.** Time dependence of the grain size parameters,  $l$  (squares) and  $w$  (circles), after quenching SI(4-13) from 70 °C (disordered state) to 52.0 °C (ordered state). The front propagation velocities are estimated by linear regression through the data obtained before  $t = 550$  min (dashed lines).

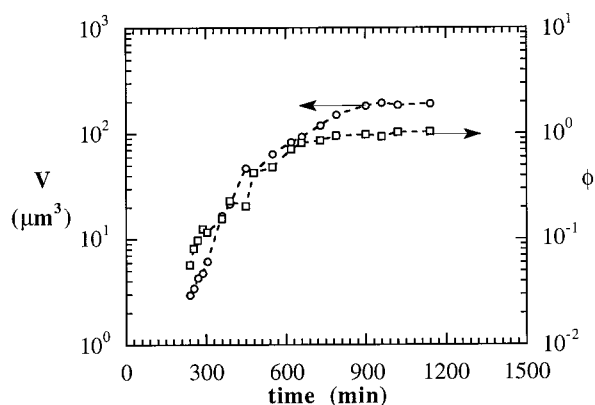


**Figure 2.** The time dependence of the grain volume,  $V$ , and grain volume fraction,  $\phi$ , after quenching SI(4-13) from 70 °C (disordered state) to 52.0 °C (ordered state).

and concentration) was derived in ref 7. At 50.0 °C we found grains with one characteristic length scale ( $w$ ). At other temperatures, the grains were ellipsoidal (on average) and thus characterized by two length scales,  $l$  and  $w$ .<sup>7-10</sup> At some temperatures (50.0 and 55.5 °C) the scattered intensity was a monotonic function of scattering angle, indicating the presence of individual ordered grains. At other temperatures (52.0 and 53.7 °C) the scattering data indicated the presence of orientation correlations within ordered domains. Ordered domains with orientation correlations may be viewed as composite grains with internal defects.<sup>7</sup>

Typical results obtained for the time dependence of  $l$  and  $w$  are shown in Figure 1 where data obtained at a quench temperature of 52.0 °C are shown. It is evident that  $l$  and  $w$  increase linearly with time during the early stage of grain growth ( $t < 500$  min). The time dependence of the average grain volume,  $V$ , and volume fraction,  $\phi$ , occupied by grains are shown in Figure 2, where  $V(t)$  and  $\phi(t)$  are shown for the 52.0 °C quench. In the early stages of grain growth ( $t < 600$  min), we observe nearly parallel trends for the time dependence of  $V$  and  $\phi$ . This implies that the increase in the volume fraction occupied by grains is primarily due to the growth of existing grains and not due to the formation of new grains. At the earliest times when grain growth is detectable ( $t = 250$  min), only 5% of the sample volume is occupied by grains. It is therefore appropriate to view the ordering process during the early stages as one where individual ordered domains grow at the

**Table 1.** Experimentally Determined Front Propagation Velocities,  $dw/dt$  and  $d/dt$  and Molecular Relaxation Time,  $\tau$ , in SI(4-13)

temp (°C)	$dw/dt$ ( $\mu\text{m}/\text{min}$ )	$d/dt$ ( $\mu\text{m}/\text{min}$ )	time range over which propagation velocity is approximately constant (min)	$\tau$ (min)
50.0	$3.5 \times 10^{-3}$	$3.5 \times 10^{-3}$	260–460	1.520
52.0	$1.2 \times 10^{-2}$	$6.1 \times 10^{-3}$	240–550	0.548
53.7	$1.1 \times 10^{-2}$	$6.4 \times 10^{-3}$	220–520	0.220
55.5	$1.5 \times 10^{-2}$	$4.4 \times 10^{-3}$	300–800	0.117

expense of the surrounding disordered phase. The ordering kinetics at a given temperature is characterized by the rate at which the ordered front propagates into the disordered phase, i.e.,  $d/dt$  and  $dw/dt$ . Estimates of  $d/dt$  and  $dw/dt$  were obtained by linear regression of the time dependence of  $l$  and  $w$  during the early stages, and these results are given in Table 1.

The rheological characterization of SI(4-13) was carried out in a Rheometrics ARES melt state rheometer with 25 mm parallel plates, using a 200 g·cm transducer with a lower sensitivity limit of 0.2 g·cm, under a nitrogen atmosphere. The polymer was placed on the bottom plate, heated to 70 °C, and allowed to flow. Under these conditions, a bubble-free sample was obtained in less than half an hour. The top plate was then slowly brought in contact with the sample. The elastic and loss moduli ( $G'$  and  $G''$ , respectively) of SI(4-13) were measured at several temperatures between 75 and 52 °C. The measurements of  $G'$  and  $G''$  at a given frequency and temperature were repeated at least two times. The strain amplitude was varied between 0.1% and 30%, depending on the magnitude of the signal (details are given below). The rheological properties, in the entire experimental range of frequencies and temperatures, were independent of strain amplitude; i.e., the measurements were made in the linear viscoelastic regime. For clarity, only one of the data sets is presented in this paper.

The experimental protocol for temperatures above and below 59 °C (the order–disorder transition temperature) were different. The rheological properties above 59 °C were independent of time and thermal history, as expected. Acquiring the data in this temperature range was therefore straightforward. Strain amplitudes of up to 30% were used, owing to the low viscosity of SI(4-13) at these temperatures. The rheological properties below 59 °C were dependent on time and thermal history, due to the formation of the ordered phase. We were mainly interested in characterizing the metastable, disordered fluid at temperatures below 59 °C. Our theoretical model (see next section) makes a particularly simple estimate of the mobility of the chains in the cylindrical phase. We assume that due to the proximity of the order–disorder transition, the order is sufficiently weak that the chain mobility may be estimated by the value in the disordered state. Experimental support for this assumption comes from the lack of a discontinuity in the chain self-diffusion coefficient at the order–disorder transition.<sup>11,12</sup>

The light scattering results described in Figure 2 indicate that the volume fraction of the ordered phase, after quenching the sample from 70 to 52 °C, was less than 3% at  $t = 200$  min. Similar results were obtained at other temperatures between 50 and 56 °C.<sup>7</sup> In this paper, we only discuss rheological data obtained during the first hour after quenching the sample from 70 °C to the temperature of interest. Extrapolations of our light scattering data indicate that the volume fraction of the

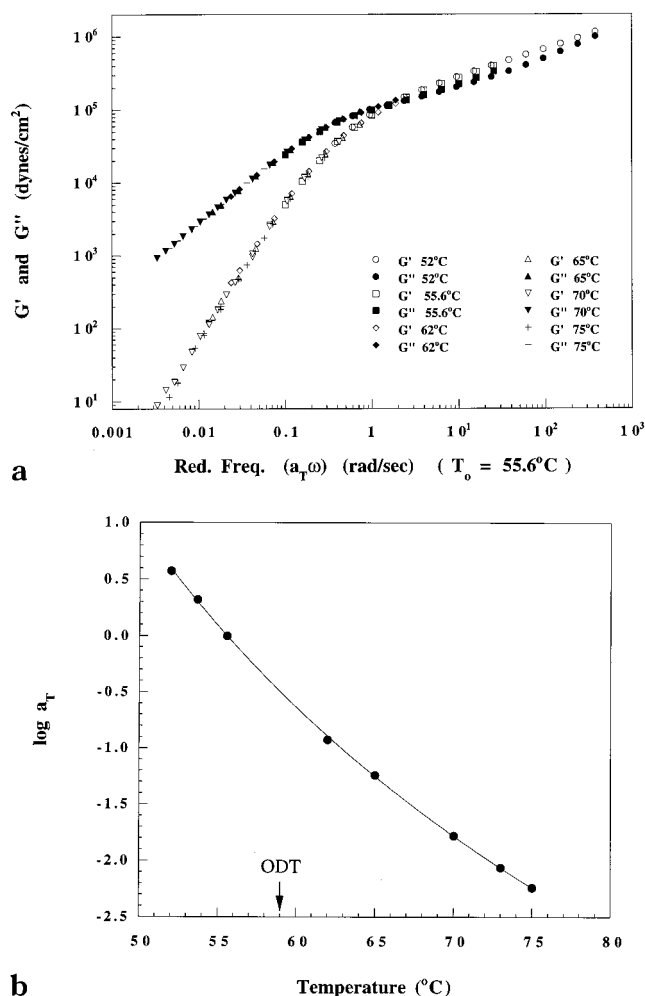


**Figure 3.** (a) Dependence of the elastic and loss moduli ( $G'$  and  $G''$ , respectively) of disordered SI(4-13) at 55.6 °C; master curve obtained by time-temperature superposition. The measurements at and below 55.6 °C were carried out during the first 60 min after quenching into the ordered state, before significant ordering could take place. The rheological response of the sample at the higher temperatures were independent of time due to the fact that the sample was disordered. (b) Temperature dependence of the horizontal shift factors  $a_T$  used to obtain the master curve shown in part a. The order-disorder transition temperature (ODT) is shown on the figure.

ordered phase during this time is negligible. The rheological signal is therefore dominated by the viscoelastic response of the disordered fluid. In addition, we kept the strain amplitude  $\leq 1\%$ , because the application of large strains is known to induce order in block copolymers. We found that the rheological properties measured under these circumstances were entirely reproducible, and independent of time and thermal history. After a few hours (at temperatures  $\leq 56$  °C), however, we found a sharp increase in  $G'$  and  $G''$ , due to viscoelastic contributions of the ordered state. We do not discuss these data in this paper.

The rheological data obtained at different temperatures exhibited time-temperature superposition. Only a horizontal shift was applied. The master curves for  $G'$  and  $G''$  obtained from measurements between 75 and 52 °C, at a reference temperature of 55.6 °C, are shown in Figure 3a. Terminal behavior ( $G' \sim \omega^2$  and  $G'' \sim \omega$ ) is seen at reduced frequencies less than 1 rad/s, indicating liquidlike behavior on time scales greater than about 1 s. Typical signatures of strong chain entanglement, such as a plateau in  $G'$  or a peak in  $G''$ , are not evident

in Figure 3a. The rheological properties of the SI(4-13) melt therefore bear some resemblance to the predictions of the Rouse model.<sup>13</sup> There are, however, subtle differences between the measured data and the model. For example, the crossing of  $G'$  and  $G''$  that was observed in the experiments is inconsistent with the Rouse model. These characteristics are typical of a lightly entangled polymer melt.<sup>13</sup> The entanglement molecular weight of polystyrene is 18 kg/mol, while that of polyisoprene is 5 kg/mol.<sup>13,14</sup> The polystyrene block molecular weight in SI(4-13) is thus below the entanglement molecular weight, while the polyisoprene block molecular weight in SI(4-13) is above the entanglement molecular weight. It is therefore not entirely surprising that the rheological properties of SI(4-13) are reminiscent of lightly entangled homopolymers. For lightly entangled homopolymers, the longest relaxation time of the chains,  $\tau$ , is obtained by extrapolating the  $G'$  and  $G''$  vs  $\omega$  lines (log-log plot), in the terminal regime, and locating the  $\omega_{\text{int}}$ , the value of  $\omega$  where these lines intersect.<sup>13</sup> The value of  $\tau$  lies between  $2/\omega_{\text{int}}$  and  $3/\omega_{\text{int}}$ , depending on the extent of entanglement. We use  $\tau = 2/\omega_{\text{int}}$ , because the extent of entanglement in SI(4-13) is very small. (It will be seen that using  $\tau = 3/\omega_{\text{int}}$  does not change any of the conclusions of this paper.) This gives  $\tau = 7$  s at 55.6 °C.

The temperature dependence of the shift factors,  $a_T$ , used to obtain the superposition in Figure 3a, is shown in Figure 3b. The curve through the data gives the best fit of the Williams-Landel-Ferry (WLF) equation.<sup>13</sup> The fact that a smooth curve goes through the data acquired above and below 59 °C lends support to the notion that the measurements below 59 °C are dominated by the viscoelastic response of the metastable, disordered fluid. The WLF analysis gives the temperature dependence of  $\tau$ :

$$\log a_T = \log \frac{\tau(s)}{7} = \frac{-7.4(T - 55.6)}{42.0 + T - 55.6} \quad (T \text{ in } ^\circ\text{C}) \quad (1)$$

Estimates of the molecular relaxation time in the metastable, disordered fluid, at temperatures between 50 and 56 °C, were calculated using eq 1, and the results are given in the last column in Table 1. We were able to obtain unambiguous estimates of  $\tau$  due to the simplicity of the viscoelastic properties of SI(4-13) in the stable and metastable disordered states. This may not be possible in other systems where nonterminal behavior is observed in the (stable) disordered state.

Small angle neutron scattering (SANS) experiments on SI(4-13) were conducted on the NG5 beam line at the National Institute of Standards and Technology at Gaithersburg, Maryland. The results of these experiments were published in ref 5 where scattering data from a series of polystyrene-*block*-polyisoprene copolymers, including SI(4-13), were presented. The dependence of the SANS intensity on the scattering vector,  $q$  [ $q = 4\pi \sin(\theta/2)/\lambda$ , where  $\theta$  is the scattering angle and  $\lambda$  is the wavelength of the incident neutrons], from the disordered melt was in agreement with the mean-field predictions of Leibler.<sup>1</sup> In SI(4-13), a single scattering peak was observed at  $q = q^* = 0.042 \text{ \AA}^{-1}$  at 80 °C (disordered state). This information can be used to estimate  $R_g$ , the radius of gyration of the SI(4-13) chains. The volume fraction of polystyrene in SI(4-13),  $f$ , is 0.23, and for this composition, the scattering maximum is located at  $q^* = 2.08/R_g$ .<sup>1</sup> Thus,  $R_g = 50 \text{ \AA}$ , and the root-mean-square end-to-end distance of the



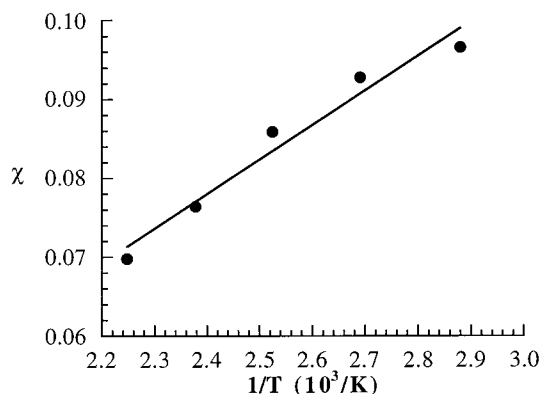


**Figure 4.** Dependence of the Flory–Huggins interaction parameter,  $\chi$ , on absolute temperature,  $T$ , measured by SANS on a melt of SI(4-13), based on a reference volume,  $v_o$ , of 150.3 Å<sup>3</sup>. The line is the result of linear regression.

chain,  $R = 6^{1/2}R_g = 122$  Å. It was reported in ref 5 that  $q^*$  obtained from SI(4-13) increased slightly with increasing temperature;  $dq^*/dT = 5 \times 10^{-5}$  (1/Å K). This corresponds to a 4% change in  $q^*$  in the temperature range between 80 and 50 °C. In this paper, we ignore the weak temperature dependence of  $R_g$ .

The Flory–Huggins interaction parameter between polystyrene and polyisoprene chains,  $\chi$ , was determined by fitting the SANS data from SI(4-13) to the theory of Leibler [see ref 5 for details]. The temperature dependence of  $\chi$  is shown in Figure 4 and is reasonably consistent with the following expression:

$$\chi = -0.027 + 43.8/T \quad (T \text{ in K}) \quad (2)$$

The  $\chi$  parameter in eq 2 is based on a reference volume,  $v_o$ , of 150.3 Å<sup>3</sup>. The number of monomers per SI(4-13) chain, based on this reference volume,  $N = 209$  (=molecular volume/ $v_o$ ). Note that the amplitude of the concentration fluctuations in SI(4-13) changes rapidly in the vicinity of the ODT (59 °C).<sup>5</sup> The SANS data shown in Figure 4 are a clear indication of this fact. However, this change in sample microstructure does not introduce rheological complexity, as indicated by the lack of nonterminal behavior (Figure 3a), and the smooth WLF dependence of the shift factors above and below the ODT (Figure 3b).

## Theory

The aim of this section is to calculate front propagation velocity in the linear regime (see Figure 1). We begin with a stable disordered phase which is quenched into a state where the cylindrical phase is stable. We assume that the quench is such that the disordered phase is metastable. In this case, the cylindrical phase invades the disordered phase by processes of nucleation and growth. We interpret the constant velocity regime in the early stages of the experiment as corresponding to such a growth process.

To identify the region of metastability we shall need to compute two spinodals on either side of the disorder–cylinder phase boundary. We shall do this within a mean-field framework. We then compute the velocity of a front propagating into a disordered phase which leaves behind it cylindrical order. We shall follow the approach of Goveas and Milner<sup>15</sup> (see ref 15 for additional details).

The experiment is carried out in a region of the phase diagram where fluctuation corrections are signifi-

cant.<sup>1,5,16</sup> Within the mean field, the BCC sphere phase is an intermediate in the transition from disorder to cylinders. When fluctuation effects are accounted for, it becomes possible to directly access the cylindrical phase from the disordered phase. Indeed, the location of both the cylinder–disorder phase boundary and the associated spinodals shift as a result of these corrections. Since our aim here is to make a simple estimate of the front velocity, we shall use mean-field theory for the cylinder–disorder transition and disregard the intervening BCC sphere phase. Also in the interest of simplicity, we ignore the anisotropic character of the front propagation and any correlations of orientational order within the domains.

**Free Energy Expansion.** Within mean-field theory the phase diagram for block copolymer melts can be described in terms of two parameters,  $\chi N$  and  $f$  (the volume fraction of the A block). The order–disorder transition is known to be weakly first-order with a critical point at  $f = 0.5$ .<sup>1,16</sup> Close to the ordering transition, a dominant wave vector with magnitude  $q^*$  appears in the system. At the limit of stability of the disordered phase, the scattering power  $S(q^*)$  diverges. This order–disorder spinodal  $(\chi N)_s$  depends only on  $f$  and is calculated in ref 1. Thus for asymmetrical copolymers where  $\chi N$  is close to  $(\chi N)_s$ , it is reasonable to describe the ordering transition by taking into consideration only the wave vectors with component  $q^*$ . This regime is known as the weak-segregation limit and produces an ordered phase with periodicity  $2\pi/q^*$ , which is on the order of the radius of gyration of the copolymers.<sup>1</sup>

Within this one-harmonic approximation, the free energy of the cylindrical phase may be written as an expansion of the order parameter. Here the order parameter is the average deviation from the uniform distribution of A and B monomers,<sup>1</sup> which vanishes in the disordered state but is nonzero when cylindrical order is present. The local free energy density for the disordered state is taken to be zero while that for the cylindrical state is written as<sup>1</sup>

$$F_{\text{cyl}}N/k_B T = -2[\chi N - (\chi N)_s]\psi^2 + b\psi^3 + c\psi^4 \quad (3)$$

[From now on  $k_B T$  is taken to be unity.] Here  $\psi$  is a scalar quantity denoting the amplitude of the order parameter of the cylindrical phase, which is zero for the disordered phase.

The coefficients in the expansion are calculated using the random phase approximation (RPA), which assumes that the chains are only slightly perturbed from being random coils. Here  $b = 2\Gamma_3/3\sqrt{3}$ ,  $c = (\Gamma_4(0,0) + \Gamma_4(0,1))/12$ ; the  $\Gamma_i$ 's are only functions of  $f$  and their explicit form is given in ref 1.

Minimizing  $F$  with respect to  $\psi$  gives the amplitude  $\psi_{\text{min}}$  for an equilibrium cylindrical phase at a fixed  $\chi N$ . At coexistence

$$\psi_{\text{min,ODT}} = b/2c \quad (4a)$$

$$(\chi N)_{\text{ODT}} - (\chi N)_s = -b^2/8c \quad (4b)$$

**Calculating the Spinodals.** Since we only consider perturbations with wave vector  $q^*$  the limit of stability of the disordered phase  $(\chi N)_{\text{disorder}}$  with respect to the cylindrical phase is just  $(\chi N)_s$ . Let us denote the limit of stability of cylinders with respect to disorder by  $(\chi N)_{\text{cyl}}$

which is given by

$$\left. \frac{\partial^2 F_{\text{cyl}}}{\partial \psi^2} \right|_{\psi=\psi_{\min}} = 0 \quad (5)$$

Using eq 3 gives

$$(\chi N)_{\text{cyl}} - (\chi N)_s = \frac{3b\psi_s + 4c\psi_s^2}{4} \quad (6)$$

where the amplitude of equilibrated cylinders at the spinodal is

$$\psi_s = -\frac{3b}{8c} \quad (7)$$

It is important to keep in mind that incorporating fluctuation corrections<sup>16</sup> predicts *no* stability limit for the disordered phase, although in practice the nucleation barrier is sufficiently small that the metastable state decays rapidly simply due to thermal fluctuations. In the following sections, we investigate front propagation close to coexistence, which is not affected by the actual position of the spinodals.

**Front Propagation.** Let us now consider a front propagating from the cylindrical phase into the disordered phase close to coexistence. The system evolves in time by means of an interface that moves in space into a higher energy state from a lower energy one. The front is described by  $\psi(z, t)$ , where  $\psi = \psi_{\min}$  at  $z = -\infty$ ,  $\psi = 0$  at  $z = +\infty$ , and the interface is located at  $z = 0$ .

Since  $\psi$  is not a conserved variable we write a dynamic equation for it, having the form

$$\Gamma \frac{d\psi}{dt} = -\frac{\delta H}{\delta \psi} \quad (8)$$

Here the energy released by the system in reducing its free energy (given by the right-hand side) is dissipated by drag forces given by the terms on the left-hand side, where  $\Gamma$  is a "drag coefficient".

We express the effective Hamiltonian  $H$  as a sum of two terms, a local part given by eq 3, and square gradient terms reflecting the free energy cost to create interfaces in the system

$$H = k_B T \int \frac{d^3 r}{v_0} [a_0^2 (\nabla \psi)^2 + F(\psi)] \quad (9)$$

where  $a_0$  is a monomeric length and  $v_0$  is a monomeric volume. More complicated and realistic expressions may be written for both eqs 8 and 9,<sup>15</sup> but we shall only consider the simplest case here. For example, our analysis may be generalized to account for grain growth anisotropy by using different values for  $a_0$  in the square gradient terms of the Hamiltonian, depending on the direction of the interface normal with respect to the ordering direction.

To estimate  $\Gamma$ , consider the relaxation of a cylindrical fluctuation in the disordered phase. [Since the system is weakly segregated it is reasonable to estimate the drag coefficient by its value in the disordered phase.] Expanding the right-hand side of eq 9 to first order, we see that the solution of eq 8 has the form  $\exp[4(\chi N - (\chi N)_s)\tau/(\Gamma v_0 N)]$ . For a disordered phase with  $\chi N$  equal to zero, the dynamics are simply those of homopolymer chains which relax on a time scale given by the longest

relaxation time,  $\tau$ , corresponding to the Rouse time or the disengagement time for unentangled and entangled chains, respectively.<sup>13,17</sup> This means that  $\Gamma$  is approximately given by  $4(\chi N)_s \tau / v_0 N$ . [Later on we shall use a more accurate expression for  $\Gamma$  to calculate the front velocity.]

**Front Velocity.** Taking our cue from the experiment let us assume that the front propagates along one dimension ( $z$ ), with a constant velocity so  $\psi(z, t) = \psi(z - vt)$ . The governing equation for isotropic front propagation becomes

$$-\Gamma v \frac{d\psi}{dz} = \frac{2a_0^2}{v_0} \frac{d^2\psi}{dz^2} - \frac{1}{v_0} \frac{dF}{d\psi} \quad (10)$$

Equation 10 also describes a classical particle of mass  $2a_0^2/v_0$  moving in an external potential  $-F(\psi)$  with friction coefficient  $\Gamma v$ . Here  $z$  plays the role of time, and  $\psi$  is the particle position. Let us say that the particle starts at an infinitesimally small velocity at a very early time at  $-F(0)$  and comes to rest at  $-F(\psi_{\min})$ . On physical grounds, there is only one value of friction coefficient  $\Gamma v$  that will dissipate the kinetic energy gained as the particle falls from the higher maximum to the lower one.

The analogous initial condition in front propagation is a nearly constant value of the order parameter at a minimum of  $F(0)$  far removed from the front. For the system to evolve into the state given by the lower minimum of  $F(\psi_{\min})$ , there is a unique front velocity at which the front will propagate.

To solve for the front velocity, we multiply both sides of eq 10 by  $d\psi/dz$  and integrate over all space

$$v = -\frac{1}{\Gamma v_0} \frac{F(\psi_{\min})}{\int_{-\infty}^{+\infty} dz (d\psi/dz)^2} \quad (11)$$

where we have used the fact that gradients in  $\psi$  vanish far from the interface.

To evaluate the integral in the denominator we change variables to  $\psi$ . At coexistence there is no front motion, so the left-hand side of eq 10 is set to zero which gives

$$\frac{d\psi}{dz} = \frac{1}{a_0} F(\psi)^{1/2} \quad (12)$$

Substituting eq 12 into eq 11 above gives

$$v = \frac{a_0}{\Gamma v_0} \frac{F(\psi_{\min})}{\int_0^{\psi_{\min}} d\psi F(\psi)^{1/2}} \quad (13)$$

At coexistence  $F(\psi)$  has two minima, so we can rewrite it as a quartic having the form

$$F(\psi) = \frac{e}{N} \left[ \left( \frac{2\psi}{\psi_{\min}} - 1 \right)^2 - 1 \right]^2 \quad (14)$$

where  $e = c\psi_{\min}^4/2$ .

Using this in eq 13 gives the following equation for the front velocity:

$$v = -\frac{a_0 N^{1/2}}{\Gamma v_0} \frac{3F(\psi_{\min})}{2e^{1/2}\psi_{\min}} \quad (15)$$

We evaluate all terms in eq 15 at coexistence except  $F(\psi_{\min})$  which we expand about its value at coexistence. This gives us the final result for the velocity as

$$v = \frac{a_0}{\Gamma \nu_0 N^{1/2}} [\chi N - (\chi N)_{\text{ODT}}] \left[ \frac{-24c^{1/2}}{b} \right] \quad (16)$$

The rheological data obtained from SI(4-13) in the disordered state showed it to be a very lightly entangled polymer melt. It is therefore more appropriate to describe its dynamics with the Rouse model rather than using reptation dynamics. Using Liebig and Fredrickson's<sup>18</sup> expression for  $\Gamma$  for Rouse chains, we obtain  $\Gamma = h(f)\tau/(2\nu_0 N)$  where  $h(f)$  is a function independent of  $\chi N$ . Then

$$v \approx \frac{R}{\tau} [\chi N - (\chi N)_{\text{ODT}}] g(f) \quad (17)$$

where  $R$  is the root mean-square end-to-end distance of the chain. The physical meaning behind eq 17 is clear: the characteristic scale for the velocity is set by the ratio of the available length and time scales, the chain radius of gyration, and the chain relaxation time, respectively. Since at coexistence, the growth rate must be zero, the growth velocity sufficiently close to the coexistence is linear in the parameter  $[\chi N - (\chi N)_{\text{ODT}}]$ . For  $f = 0.23$ , which is the case for SI(4-13),  $g(f) = 0.575$ . For other ordering transitions, the main difference will arise in the factor  $g(f)$ , which depends only on copolymer composition.

### Comparing Theory and Experiment

We make the velocity dimensionless by dividing by the characteristic scale of the velocity, i.e.,  $v^* = v(\tau/R)$ . If we approximate the temperature dependence of  $\chi$  in the usual way,  $\chi = A + B/T$ , then we obtain the following expression for the temperature dependence of the dimensionless front velocity by substituting eq 2 into eq 17:

$$v^* = NBg(f) \left[ \frac{1}{T} - \frac{1}{T_{\text{ODT}}} \right] \quad (18)$$

To compare theory and experiment, we scale the experimentally determined front propagation velocities by the characteristic velocity  $R/\tau$  (see Table 1) to obtain  $v_L^*$  and  $v_W^*$ :

$$v_L^* = \frac{dl}{dt} \frac{\tau}{R} \quad (19a)$$

$$v_W^* = \frac{dw}{dt} \frac{\tau}{R} \quad (19b)$$

In Figure 5 we plot the experimentally determined  $v_L^*$  and  $v_W^*$  as a function of  $[1/T - 1/T_{\text{ODT}}]$ . While we have plotted our results in terms of the temperature relative to the order-disorder transition, it is important to realize that the parameter driving front propagation

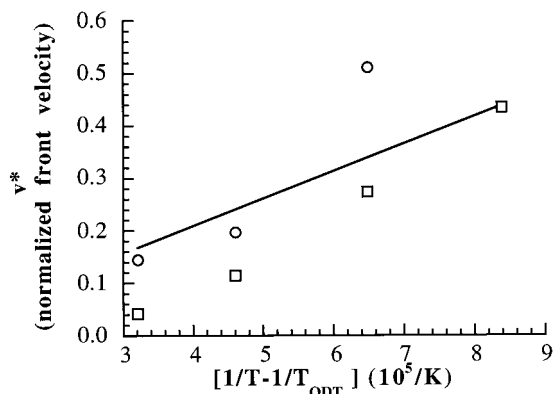


**Figure 5.** Experimentally determined normalized front propagation velocity,  $v^*$ , vs quench depth,  $[1/T - 1/T_{\text{ODT}}]$ . Key circles,  $v_L^*$ ; squares,  $v_W^*$ ; line, theoretical prediction.

is the difference in  $\chi N$  from the order-disorder transition. The line in Figure 5 represents the theoretical prediction for the dependence of  $v^*$  on  $[1/T - 1/T_{\text{ODT}}]$  which is a straight line through the origin with slope =  $NBg(f) = 5228$ . It is evident that the experimental measurements of grain growth velocity in the linear regime are in good agreement with the theoretical predictions with no adjustable parameters.

### Concluding Remarks

The ordering kinetics in a block copolymer melt, following a thermal quench from the disordered state, were studied by depolarized light scattering. Ordered grains nucleated and grew by consuming the surrounding disordered phase. The growth rate of the grains is characterized by the velocity at which the front of the ordered phase propagates into the disordered phase. We derived an expression for the dependence of this front propagation velocity on quench depth, molecular size, and molecular relaxation time. Independent estimates of these parameters were made using SANS and rheological measurements. The magnitudes of the experimentally determined front velocities were in good agreement with our theoretical predictions, with no adjustable parameters.

To our knowledge, such a stringent comparison between theory and experiment has not been affected in studies of ordering kinetics in other systems. Block copolymer melts are model materials for studying ordering kinetics from both experimental and theoretical points of view. Volume changes and heat effects associated with the disorder-to-order transition in block copolymers are negligible.<sup>19,20</sup> They remain highly transparent during all stages of grain growth. Single scattering theories can therefore be used to determine the grain structure from scattering data.<sup>7,8</sup> The high viscosity of the disordered phase leads to slow kinetics, facilitating experimental measurements. In addition, robust, molecular theories for describing equilibrium thermodynamics are available.

In identifying the important parameters and scales in characterizing the ordering kinetics, the theoretical model leaves out finer features such as fluctuation corrections to the free energy, anisotropic grain growth, the presence of defects, and the effect of light entanglement. Also, our theory aims only to describe the initial stages of grain growth where isolated grains grow independently. At later times, the growth becomes

nonlinear due to interactions between grains. Addressing these intriguing aspects of the kinetics will require richer dynamical models than are currently available.<sup>15,21,22</sup> It will be interesting to see if the agreement between theory and experiment holds for other block copolymer ordering transitions. It is also desirable to probe ordering kinetics by other experimental methods such as small-angle X-ray and neutron scattering.<sup>23-25</sup> We believe, however, that this work represents a step toward identifying the factors that govern the kinetics of order formation in block copolymer melts.

**Acknowledgment.** We thank Glenn Fredrickson, Scott Milner, and Hiroshi Watanabe for educational discussions. Financial support from the National Science Foundation (DMR-9457950) and Research Corporation is gratefully acknowledged. Acknowledgment is made to the donors of the Petroleum Research Fund, administered by the American Chemical Society, for support of this research.

## References and Notes

- (1) Leibler, L. *Macromolecules* **1980**, *13*, 1602.
- (2) de Gennes, P. G.; Prost, J. *The Physics of Liquid Crystals*, 2nd ed.; Oxford: New York, 1993.
- (3) Seul, M.; Andelman, D. *Science* **1995**, *267*, 476.
- (4) Hohenberg, P. C.; Halperin, B. I. *Rev. Mod. Phys.* **1977**, *49*, 435.
- (5) Lin, C. C.; Jonnalagadda, S. V.; Kesani, P. K.; Dai, H. J.; Balsara, N. P. *Macromolecules* **1994**, *27*, 7769.
- (6) Perahia, D.; Vacca, G.; Patel, S. S.; Dai, H. J.; Balsara, N. P. *Macromolecules* **1994**, *27*, 7645.
- (7) Newstein, M. C.; Garetz, B. A.; Balsara, N. P.; Chang, M. Y.; Dai, H. J. *Macromolecules* **1998**, *31*, 64.
- (8) Dai, H. J.; Balsara, N. P.; Garetz, B. A.; Newstein, M. C. *Phys. Rev. Lett.* **1996**, *77*, 3677.
- (9) The asymmetry of the underlying cylindrical structure implies that the interfacial free energy between the ordered grains and the surrounding disordered fluid depends on the orientation of the microstructure relative to the interface. This anisotropy in interfacial free energy will lead to anisotropic grains if the grains are grown at a temperature that is sufficiently close to the coexistence temperature. However, at large quench depths, the kinetics of grain growth may be relatively rapid, and the observed grain shapes will be affected by kinetic factors as well as thermodynamic factors. A model for predicting equilibrium grain shapes in ordered block copolymers will be published soon.<sup>10</sup>
- (10) Marques, C. M.; Balsara, N. P. Manuscript in preparation.
- (11) Shull, K. R.; Kramer, E. J.; Bates, F. S.; Rosedale, J. H. *Macromolecules* **1991**, *24*, 1383.
- (12) Balsara, N. P.; Stepanek, P.; Lodge, T. P.; Tirrell, M. *Macromolecules* **1991**, *24*, 6227.
- (13) Ferry, J., *Viscoelastic Properties of Polymers*, 3rd ed.; Academic Press: New York, 1980.
- (14) Fetters, L. J.; Lohse, D. J.; Colby, R. H. Chapter 24 In *Physical Properties of Polymers Handbook*; Mark, J. E., Ed.; AIP Press: Woodbury, New York, 1996.
- (15) Goveas, J. L.; Milner, S. T. *Macromolecules* **1997**, *30*, 2605.
- (16) Fredrickson, G. H.; Helfand, E. *J. Chem. Phys.* **1987**, *87*, 697.
- (17) Doi, M.; Edwards, S. F. *The Theory of Polymer Dynamics*; Oxford: New York, 1986.
- (18) Liebig, C. M.; Fredrickson, G. H. *J. Polym. Sci.: Part B* **1996**, *34*, 163.
- (19) Hajduk, D. A.; Gruner, S. M.; Erramilli, E.; Register, R. A.; Fetters, L. J. *Macromolecules* **1996**, *29*, 1473.
- (20) Stuhn, B. *J. Polym. Sci.: Part B* **1992**, *30*, 1013.
- (21) Fredrickson, G. H.; Binder, K. *J. Chem. Phys.* **1989**, *91*, 7265.
- (22) Qi, S.; Wang, Z. G. *Phys. Rev. Lett.* **1996**, *76*, 1679.
- (23) Harkless, C. R.; Singh, M. A.; Nagler, S. E.; Stephenson, G. B.; Jordan-Sweet, J. L. *Phys. Rev. Lett.* **1990**, *64*, 2285.
- (24) Hashimoto, T.; Sakamoto, N. *Macromolecules* **1995**, *28*, 4779.
- (25) Hajduk, D. A.; Tepe, T.; Takenouchi, H.; Tirrell, M.; Bates, F. S. *J. Chem. Phys.* **1998**, *108*, 326.

MA980457H